Nanoscale

RSC Publishing

PAPER

View Article Online
View Journal | View Issue

Cite this: *Nanoscale*, 2013, **5**, 6851

A self-heated silicon nanowire array: selective surface modification with catalytic nanoparticles by nanoscale Joule heating and its gas sensing applications†

Jeonghoon Yun,[ab] Chun Yan Jin,[ab] Jae-Hyuk Ahn,[ab] Seokwoo Jeon[bc] and Inkyu Park*[ab]

Received 2nd April 2013
Accepted 20th May 2013

DOI: 10.1039/c3nr01640d

www.rsc.org/nanoscale

We demonstrated novel methods for selective surface modification of silicon nanowire (SiNW) devices with catalytic metal nanoparticles by nanoscale Joule heating and local chemical reaction. The Joule heating of a SiNW generated a localized heat along the SiNW and produced endothermic reactions such as hydrothermal synthesis of nanoparticles or thermal decomposition of polymer thin films. In the first method, palladium (Pd) nanoparticles could be selectively synthesized and directly coated on a SiNW by the reduction of the Pd precursor *via* Joule heating of the SiNW. In the second method, a sequential process composed of thermal decomposition of a polymer, evaporation of a Pd thin film, and a lift-off process was utilized. The selective decoration of Pd nanoparticles on SiNW was successfully accomplished by using both methods. Finally, we demonstrated the applications of SiNWs decorated with Pd nanoparticles as hydrogen detectors. We also investigated the effect of self-heating of the SiNW sensor on its sensing performance.

Introduction

Among various nanomaterials, silicon nanowires (SiNWs) are one of the good candidates for industrial applications due to the well-established silicon-based nanoelectronics technology. Moreover, the electrical properties of SiNWs can be easily controlled and the surface can be simply modified with chemical treatment. Therefore, there have been many studies on SiNWs for sensor applications in the last decade.[1–8] The applications range from the detection of chemical species including pH[1,2] and gases[3] to the detection of biological species such as DNA,[4] proteins,[5] cancer,[6] and viruses.[7] Due to the high surface-to-volume ratio, SiNW-based sensors have shown the detection limit down to a single-molecule level.[7]

Since a pristine SiNW does not possess significant selectivity to most chemical or biological species, surface modification steps are essential for the selective detection. The surface modification methods can be classified into two categories: global surface modification such as self-assembled-monolayer (SAM) coating[9] and local surface modification such as dip-pen lithography,[10] AFM surface modification,[11] electrostatic force lithography[12] and micro contact printing.[13,14] Although the global surface modification method provides high throughput surface modification, a local modification technique is required as the size of sensors is scaled down and the sensors are highly integrated into a small chip. In particular, sensor devices for multiplexed detection require local surface modification of the integrated nanowire array with heterogeneous functional groups. However, the low throughput issue in local surface modification methods has not yet been resolved.

In this paper, we introduce new methods for the selective surface modification of SiNWs based on nanoscale localized Joule heating. We have previously studied the nanoscale heating effects of silicon and metal nanowires and their applications as nanoscale heaters.[15,16] Our approach in this work is to utilize these nanoscale heating phenomena for selective surface reactions (*e.g.* thermal decomposition of polymer thin films or hydrothermal synthesis of metal nanoparticles) and surface modification on the SiNWs. These proposed methods provide high-throughput surface modification since self-aligned modification of SiNWs is enabled and no additional alignment process is required.

Scheme 1 depicts the schematic of these methods. In method 1, a SiNW is Joule-heated by applying a voltage in a metal precursor solution and metal nanoparticles are directly synthesized and coated on the surface of SiNW. In method 2, a polymer (*e.g.* PMMA) thin film coated on the SiNW is thermally decomposed by Joule heating of SiNW. Then, evaporation of the metal thin film and a lift-off process are used for the selective decoration of metal nanoparticles on the SiNW.

[a]*Department of Mechanical Engineering, Korea Advanced Institute of Science and Technology (KAIST), Daejeon 305-701, Korea. E-mail: inkyu@kaist.ac.kr; Fax: +82-42-350-3210; Tel: +82-42-350-3240*

[b]*KAIST Institute for the Nanocentury, Korea Advanced Institute of Science and Technology (KAIST), Daejeon 305-701, Korea*

[c]*Department of Materials Science and Engineering, Korea Advanced Institute of Science and Technology (KAIST), Daejeon 305-701, Korea*

† Electronic supplementary information (ESI) available. See DOI: 10.1039/c3nr01640d

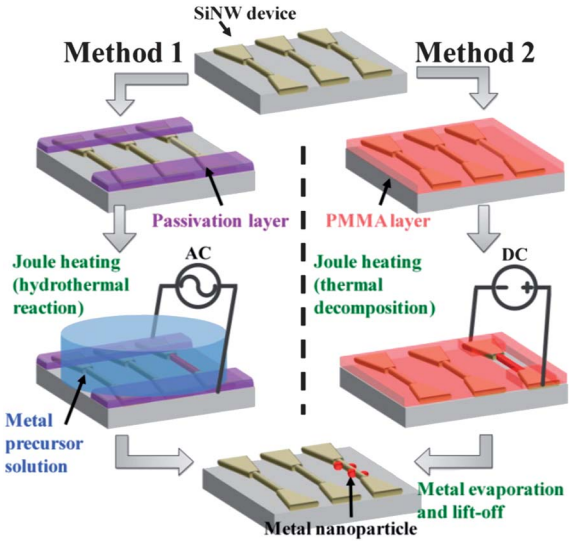

Scheme 1 Schematic description of surface modification by self-heating of a nanowire: in method 1, nanoparticles were formed by hydrothermal reaction *via* Joule heating of a SiNW. In method 2, a metal thin film was locally deposited on a SiNW through PMMA decomposition, metal evaporation and lift-off.

Experimental procedure

SiNW devices were fabricated by conventional top-down technology such as electron beam lithography (EBL) and reactive ion etching (RIE). A silicon on insulator (SOI) wafer was used as the starting substrate. The wafer had a top silicon (Si) layer with a thickness of 100 nm and a 400 nm thick buried oxide (SiO_2) layer underneath the top Si layer. By thermal oxidation and time-controlled wet etching of the oxide layer, the top Si layer was thinned down to 50 nm and covered with a 10 nm thick SiO_2 layer. Then, the SOI wafer was doped with boron ions (doping concentration: 7×10^{17} cm^{-3}) by the ion implantation process and a subsequent rapid thermal annealing process at 1000 °C for 10 seconds. SiNWs were patterned by the RIE process using a Cr layer as an etch mask which had been defined by the EBL and lift-off processes. Polymethyl methacrylate (PMMA) was used as the e-beam resist and polymethylglutarimide (PMGI, MicroChem's PMGI SF2) was used as a lift-off layer. Both PMGI and PMMA films were deposited on the SOI wafer by spin coating. A scanning electron microscope (SEM, JEOL JSM-6510) based EBL system equipped with a NPGS (Nabity System, Inc.) unit defined the geometry of nanowires 100 nm wide and 3 μm long with an acceleration voltage of 30 kV and a dose of 320 μC cm^{-2}. The patterned film was developed with a 3 : 1 (v/v) mixed solution of IPA (isopropyl alcohol) and MIBK (methyl isobutyl ketone) for 80 seconds and then transferred into IPA for 60 seconds for further developing. Dipping the samples into 60% AZ300MIF diluted by DI water for 90 seconds resulted in the undercut etching of the PMGI film for better lift-off. To remove the residual PMMA resist, an oxygen plasma process was conducted. Then, a 20 nm thick Cr layer was deposited on the nanopatterned sample by e-beam evaporation. To perform the metal lift-off process, PMMA and PMGI layers were cleaned with a PMGI remover (PG remover, MicroChem) at 100 °C for a few minutes and by subsequent ultrasonication for a few seconds. SiNWs were patterned by etching a 10 nm SiO_2 layer and a 50 nm Si layer using the RIE process (SF_6 gas) with a nanopatterned Cr layer as an etch mask. Then, the Cr layer was removed and the top SiO_2 protection layer was etched. Micro-contact electrodes were defined by aligned UV photolithography and lift-off of a 150 nm thick Al layer. The thermal annealing process was performed at 400 °C in a forming gas (a mixture of 10% H_2 and 90% N_2).

The first method (method 1 in Scheme 1) for selective surface modification of SiNW is the hydrothermal reaction of the metal precursor by nanoscale Joule heating of SiNW and is explained in the following: first, the electrodes are passivated by aligned photolithographic patterning of a photoresist and its thermal cross-linking in order to prevent unnecessary electrochemical reactions between the micro-contact electrodes and the precursor solution. In specific, a 2 μm thick photoresist (AZ NLOF 2035, AZ Electronic Materials) was deposited on a SiNW device by spin-coating at 5000 rpm and baking at 110 °C for 80 s. The layer was patterned for opening of the SiNW array by UV exposure and development of the resist. Additional baking of the passivation layer at 200 °C for 1 hour on a hot plate gave chemical resistivity due to thermal cross-linking of the photoresist. A palladium (Pd) precursor solution was prepared with a mixture of 16 mL of 1 mM K_2PdCl_4 and 200 μL of 30 mM sodium citrate.[17] An aqueous sodium hydroxide solution was added to the Pd precursor solution to set pH = 11. For further prevention of the electro-chemical reaction, an alternative voltage with a sinusoidal wave form was applied on the SiNW by a function generator (33210A, Agilent) and an amplifier. The root mean square amplitude and frequency for the AC voltage were 18.8 V and 1 kHz, respectively.

Another method (method 2 in Scheme 1) is based on the selective and localized thermal decomposition of PMMA by using Joule heating of the silicon nanowire, metal layer deposition, and a lift-off process. A 40 nm thick PMMA (950 PMMA C, MicroChem) layer was deposited on a SiNW device by spin-coating at 5000 rpm and baking at 180 °C for 15 min. For the Joule heating of SiNW and thermal decomposition of PMMA, a DC potential of 60 V was applied across the nanowire for several minutes. Nanoparticles were decorated on the SiNW by depositing a very thin metal film (<2 nm) using an electron-beam evaporator and removing the PMMA layer by dipping in acetone with ultrasonication. The structure of the SiNW decorated by metal nanoparticles was characterized by field-emission scanning electron microscopy (FE-SEM, Sirion). The morphology of decomposed PMMA was measured using an atomic force microscope (AFM, Park system XE-100).

The SiNWs decorated with Pd nanoparticles by using two methods were used as hydrogen (H_2) sensors. The SiNWs were exposed to 0.5% H_2 gas made by a mixture of synthetic air (20% O_2 and 80% N_2) and 1% H_2 gas (1% of H_2 and 99% of N_2). Air and H_2 gas were flowing at the same time with a flow rate of 300 sccm each. The resistance of the Pd decorated SiNW was measured under room temperature conditions. To observe the H_2 sensing characteristics of the Pd decorated SiNW, a constant DC voltage of 0.5 V was applied across the nanowire and the

current was measured using a source meter (Keithley 2400 SourceMeter) controlled by a computer based program (LabView, National Instrument) while the nanowire was exposed to the H_2 gas and air.

Results and discussion

The Joule heating of SiNW was calculated by numerical simulation (COMSOL Multiphysics). A SiNW with a length of 3 μm, width of 100 nm, and thickness of 50 nm was located on a Si substrate (thickness of 200 μm, area of 40 μm × 40 μm) with a top silicon dioxide (SiO_2) layer (thickness of 400 nm, area of 40 μm × 40 μm) (Fig. S1†). The temperatures at the top plane of the environment and at the bottom plane of the substrate were fixed at room temperature (293.15 K) and the boundary condition for the side walls of the environment was set to be a thermal insulation because the region and power of the Joule heating of SiNW are very small. The electrical conductivity of Si doped by boron at a concentration of 7×10^{17} cm^{-3} was 1429 S m^{-1} at room temperature and the temperature dependence of the electrical conductivity was modeled as below:

$$\sigma = \sigma_0 \frac{1}{(1 + \alpha(T - T_0))}$$

where σ_0 is the electrical conductivity at room temperature, α is the temperature coefficient of resistance, T is the temperature, and T_0 is the room temperature (293.2 K). Here, α was set as 0.0002 K^{-1} for the given doping level.[18] Other material properties were employed from the database of the simulation software. An electrical bias was applied across the circuit and heat was generated by Joule heating of SiNW. The heat was mainly dissipated by conductive heat transfer to the substrate and convective heat transfer to the air or water environment above the nanowire device.

Fig. 1(a–d) show the simulation result of SiNW's Joule heating by the numerical simulation. A maximum temperature of 363 K was observed at the center of SiNW when an electrical bias of 20 V was applied. The cross-sectional temperature profile of the simulation result shows that the Joule heating of SiNW generates a highly localized heating in the nanoscale space. The maximum temperature gradient was 0.765 K nm^{-1} (= 765 K μm^{-1}) at the edge of SiNW and the temperature at a distance of 1 μm from the center of SiNW was 296.4 K which is similar to the room temperature (293.2 K). The temperature of SiNW was controlled by adjusting the applied voltage and affected by the surrounding media. Fig. 1(e–f) depict the maximum temperature of SiNW *versus* the applied electrical bias in air and water environments. The temperature of SiNW reached 100 °C in a water environment and 132 °C in an air environment when 25 V was applied on SiNW. This difference is due to a higher heat transfer coefficient and thermal capacity of water than those of air. The transient analysis shows that the temperature is saturated within hundreds of nano-seconds (Fig. 1(g)). The rise time (τ_r) required to reach from 10% to 90% of the steady-state temperature is 81.2 ns. This ultrafast thermal response originates from the small thermal capacity of the SiNW heater. The temperature of SiNW can be manipulated within a few hundred nano-seconds by applying an electrical bias and is high enough to produce endothermic chemical reactions such as thermal reduction of metal precursors and thermal decomposition of polymer thin films.

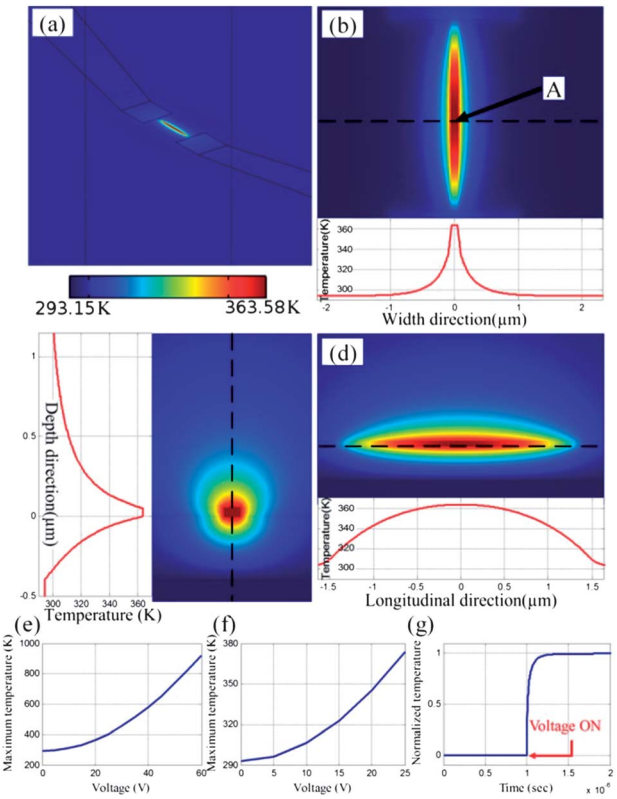

Fig. 1 Steady-state and transient temperature analysis of SiNW during Joule heating by numerical simulation: (a) three dimensional temperature distribution near Joule-heated SiNW, (b) two and one dimensional temperature profiles in the *x–y* plane on the surface of silicon oxide, (c) two and one dimensional temperature profiles in the *x–z* plane along the center of the nanowire, (d) two and one dimensional temperature profiles in the *y–z* plane along the center of the nanowire, (e–f) temperature at point A *versus* applied DC voltage in (e) an air environment and (f) a water environment, and (g) step response of the temperature at point A to a constant DC voltage.

SiNWs can be heated not only by applying a DC potential but also by applying an AC potential. In fact, an AC potential is sometimes beneficial to reduce unwanted electrochemical reactions in a liquid environment. We calculated the temporal temperature change at the center of SiNW under an AC potential with various frequencies by numerical simulation (Fig. S2†). When the AC frequency is low, the time for heating and cooling is long enough to generate a sinusoidal temperature change of the nanowire. We can observe that the frequency of temperature change is twice of the AC potential's frequency because both positive and negative potentials generate the Joule heating of the nanowire. Also, the maximum temperature achieved by an AC potential is identical to the temperature under the DC potential with the same amplitude of the AC potential. However, as the frequency of the AC potential is increased, heating and cooling of the nanowire cannot follow the fluctuation of the AC potential and therefore the maximum temperature of the

nanowire is decreased. As shown in Fig. S2,† the cutoff frequency (f_c) for the AC heating is between 1 MHz and 10 MHz. Below this frequency, the maximum temperature by the AC potential is larger than −3 dB of the maximum value by the DC potential. This frequency range is consistent with the cutoff frequency (f_c = 4.31 MHz) calculated by the formula of $f_c \sim 0.35/\tau_r$ where τ_r is the rise time (81.2 ns) in the step response.[19]

Fig. 2 shows the result of selective synthesis and decoration of Pd nanoparticles by hydrothermal reaction through Joule heating of SiNW under an AC voltage with an amplitude of 18.8 V and a frequency of 1 kHz. Pd nanoparticles with an average diameter of 42 nm and a standard deviation of 27 nm were grown on the Joule heated SiNW whereas they were not synthesized on the non-heated SiNW. Pd nanoparticles were synthesized near the center of Joule heated SiNW, which is the hottest area as calculated by the numerical simulation shown in Fig. 1(b). During this experiment, the electrochemical reaction on the metal electrodes was eliminated by the passivation layer, but electrochemical reaction on SiNW and Si electrodes could not be avoided since they were directly exposed to the reaction chemical. In order to prevent the electrochemical reaction, AC voltage was applied instead of DC voltage for Joule heating of SiNW. As mentioned above, the maximum temperature of the nanowire decreases with the increasing AC frequency. Therefore, we used AC Joule heating with a reasonable frequency (1 kHz) for heating the precursor solution to an appropriate temperature as well as for reducing the electro-chemical reaction.

Localized thermal decomposition of the polymer also enabled selective surface modification of SiNWs. As the electrical bias was applied on a SiNW, nanoscale Joule heating along the SiNW was generated and the polymer was locally decomposed. As a result, the surface of heated SiNW was opened for surface modification. For the localized thermal decomposition of the polymer, a DC bias

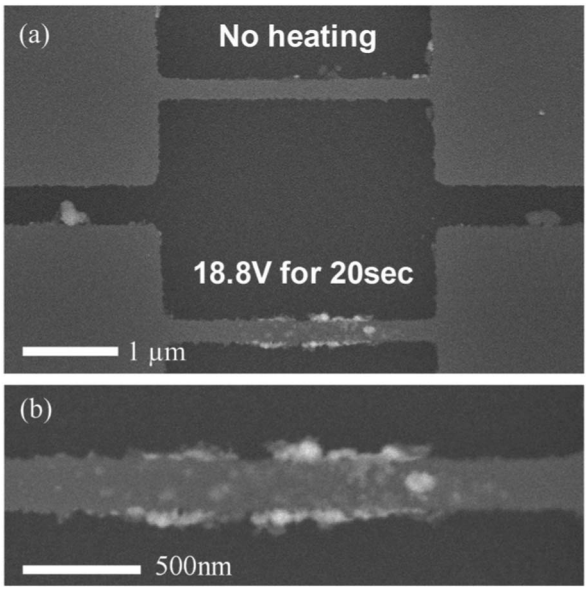

Fig. 2 SEM images of the nanoparticle decorated SiNW *via* Joule heating in a liquid metal precursor environment: (a) Pd nanoparticles selectively coated on the heated SiNW and (b) high magnification SEM image of Pd nanoparticles on the heated SiNW.

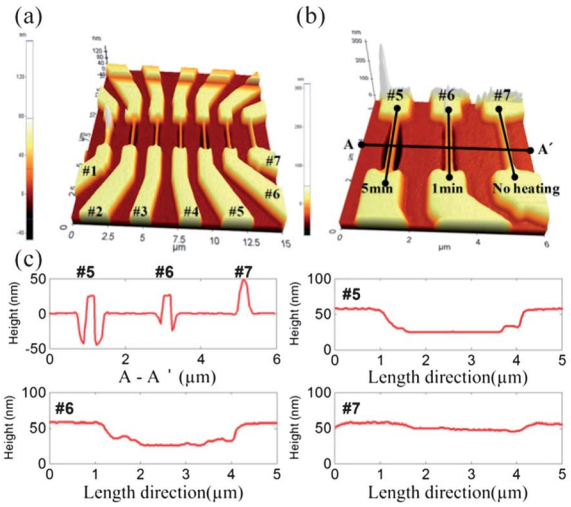

Fig. 3 Thermal decomposition of the polymer by Joule heating of SiNW: (a) AFM image of PMMA thermal decomposition by a DC voltage of 60 V across a 3 μm long SiNW for different time periods, (b) high resolution AFM image of PMMA decomposition, and (c) line profile along the *A*–*A*′ direction and length direction of nanowires #5, #6, and #7.

of 60 V was applied across a SiNW for 1 minute (nanowire #6) and 5 minutes (nanowire #5) after the coating of the PMMA layer on the device chip. Fig. 3 shows that the nanowire surface was opened by selective decomposition of PMMA. As shown in Fig. 3(c), the decomposed area was widened as the heating time was increased. This result was caused by the spreading of heat from the nanowire to surrounding, the amount of which is determined by the applied voltage and time. As shown in the line profile along the longitudinal direction of the nanowire (Fig. 3(c)), most thermal decomposition of PMMA occurred near the center region of the nanowire, whereas both ends of the nanowire were still covered with PMMA. This can be attributed to the high temperature at the center of the nanowire and the lower temperature near the edge of the nanowire caused by the heat dissipation to the electrodes, which was confirmed by the numerical simulation. This self-passivation of the electrode region is one of the attractive merits of the localized thermal decomposition of the polymer using the nanoscale Joule heating of SiNW.

As explained above, by the PMMA decomposition, evaporation of the Pd thin film and lift-off, selective coating of SiNWs with Pd nanoparticles can be realized. Fig. 4(a and b) show the SEM images of the selectively deposited Pd nanoparticles along the Joule-heated SiNW. Because of the surface tension between Pd and SiNW, Pd nanoparticles were formed rather than a continuous Pd film in the case of very small deposition thickness.[20] A multiplexed SiNW array decorated with different metals was fabricated by repeating the above mentioned selective surface modification process (*i.e.* PMMA decomposition, metal deposition and lift off) with different metals. In particular, we decorated nanowires with Au and Pd thin films. Fig. 4(c) shows the SEM image of the multiplexed SiNW array and the EDS results of metal decorated SiNWs. Au element is observed on nanowire #5 while a negligible amount of Au is observed on nanowire #6 and elsewhere. Also, Pd element is observed on nanowire #6 while it can hardly be found on

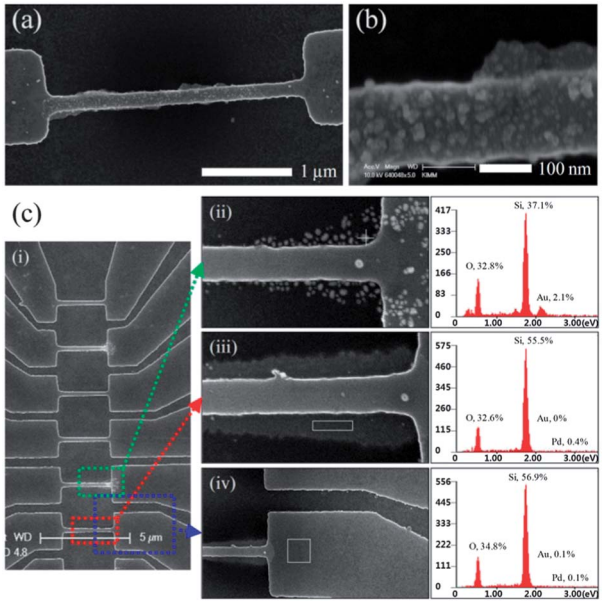

Fig. 4 Selective surface modification of SiNWs by PMMA decomposition and thermal evaporation: (a) SEM image of selective Pd decoration on a SiNW by method 2 (PMMA decomposed by applying a voltage of 60 V on the nanowire for 1 min), (b) high resolution image of (a), and (c) multiplexed SiNW array decorated with different metals (Au and Pd): (i) SEM image of the SiNW array. SEM and EDS results of (ii) gold, (iii) palladium decorated SiNW and (iv) the region without particle decoration.

nanowire #5 and elsewhere. This result verifies that each nanowire can be selectively decorated with different metals by using the method we proposed above.

Fig. 5(a) and (b) show the H_2 sensing results of SiNWs decorated with Pd nanoparticles by using methods 1 and 2, respectively. The sensitivity (S) of the SiNW was defined by $S = (R_{H_2} - R_{air})/R_{air} \times 100$ (%) where R_{air} and R_{H_2} are the resistance of the Pd-decorated SiNW in air and in H_2, respectively. The response time of the sensor was defined as the time interval between 10% and 90% increase of sensor resistance. The sensitivity and response time of the Pd-decorated SiNW sensor by using method 1 were 70% and 750 s, respectively. A sensitivity of 53% and a response time of 26 seconds were observed for Pd-decorated SiNW by method 2. Also, the H_2 response of bare SiNW was monitored to verify the effectiveness of the Pd nanoparticle coating on the H_2 sensing. As shown in Fig. 5(c), a bare SiNW does not respond to H_2 gas. Therefore, we can conclude that selective surface decoration of SiNW by Pd nanoparticles enables the sensing of the H_2 gas.

When Pd is exposed to H_2 gas, it will absorb H_2 gas and form palladium hydride (PdH_x). The coverage (θ)[17] of hydrogen atoms is a function of partial pressure of H_2 (P_{H_2}) as shown below.

$$\theta/(1 - \theta) = (k_1/k_{-1})^{1/2} P_{H_2}{}^{1/2}$$

where k_1 and k_{-1} are the absorption and desorption constants, respectively.

As the coverage of hydrogen increases, the work function of PdH_x decreases.[21] Therefore, the work function of PdH_x is also a function of P_{H_2}. When PdH_x is formed, band bending occurs by the difference of the Fermi level (E_F) between SiNW and PdH_x and thus

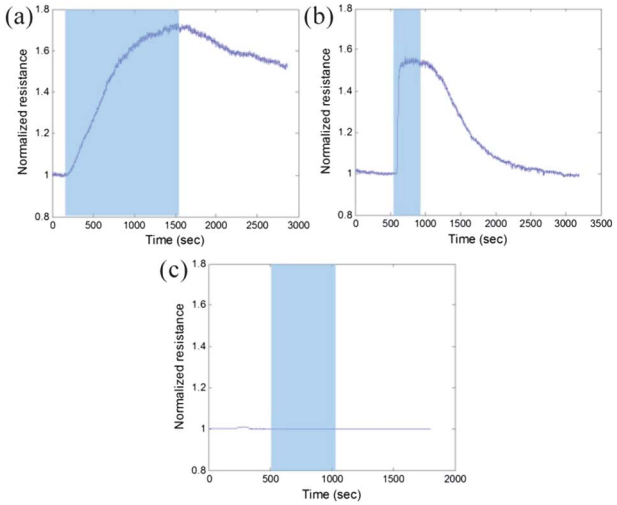

Fig. 5 Hydrogen sensing result of (a) the SiNW decorated with Pd nanoparticles by method 1, (b) the SiNW decorated with Pd nanoparticles by method 2, and (c) the bare SiNW. The blue area represents the hydrogen exposure period and other areas represent the air exposure.

the electric conductivity of the SiNW decreases due to the narrow path for the electric conduction. Therefore, when P_{H_2} increases, the electrical conductivity of Pd decorated SiNW decreases.

The self-heating of SiNWs can be used for improving the response speed of the sensor by increasing the reaction temperature. Fig. 6(a–d) show the results of H_2 sensing by Pd-decorated SiNWs (method 2) with self-heating, where 0.5% H_2 gas mixed in air was used as a target gas. Different DC voltages

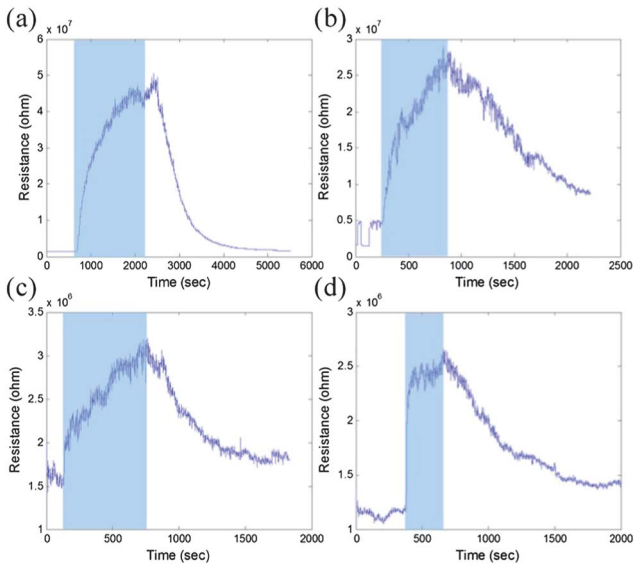

Applied voltage	0.5V	10V	20V	30V
Sensitivity (=(R_{H2}-R_{air})/R_{air}×100)	3470%	450%	100%	106%
Response time (from 10% to 90%)	930sec	400sec	385sec	24sec

Fig. 6 Hydrogen sensing with a self-heated silicon nanowire with a surface coating of Pd nanoparticles: applied voltages of (a) 0.5 V, (b) 10 V, (c) 20 V, and (d) 30 V. The blue area represents the hydrogen exposure period and other areas represent the air exposure. The sensitivity and response time of self-heated and Pd decorated silicon nanowire are summarized in the table.

(0.5 V, 10 V, 20 V, and 30 V) were applied across Pd decorated SiNW to investigate the effect of self-heating. The sensitivity and the response time with various applied voltages are summarized in a table in Fig. 6. Lower sensitivity and faster response were observed as higher voltage was applied. When an electrical bias of 30 V was applied, we could observe 32.7 times lower sensitivity but 38.8 times shorter response time than when an electrical bias of 0.5 V was applied. Also, a fast recovery of resistance was observed by applying a high electrical bias. The recovery time is defined as the time interval from the point of gas shut-off to the point of 90% of the final saturation. The recovery times were measured to be 1350 s and 590 s for 0.5 V and 30 V, respectively.

The atomic ratio of hydrogen to palladium (x) in palladium hydride (PdH_x) is a function of temperature and partial pressure of H_2. As the temperature is increased, the hydrogen content x in PdH_x is decreased.[22] Therefore, the electrical conductive path in SiNW is wider at high temperature due to the reduced difference of the work function. This means that the sensitivity at high temperature is lower than that at low temperature. However, as the temperature is increased, absorption and desorption of hydrogen occur faster due to higher kinetic energy of hydrogen. Therefore, the response and recovery times are shorter at high temperatures.

Conclusions

In summary, a novel method for selective surface modification of the SiNW array was developed in this work. Selective surface modification of a SiNW could be achieved simply by localized temperature control *via* Joule heating of the SiNW. This method does not require a tedious alignment process for selective and localized surface modification, as opposed topreviously developed methods. We expect that a high-performance, integrated, and multiplexed nanowire sensor array can be easily fabricated by using our proposed method.

Acknowledgements

This research was supported by the Basic Science Research Program (Grant No: 2012-0002021) through the National Research Foundation of Korea (NRF), Smart IT Convergence System Research Center (Grant No: 2012M3A6A6054201), and Global Frontier R&D Program (Grant No: 2011-0031563) funded by the Korean government (MEST).

References

1 I. Park, Z. Li, A. P. Pisano and R. S. Williams, *Nanotechnology*, 2010, **21**, 015501.
2 S. Choi, I. Park, Z. Hao, H. N. Holman and A. P. Pisano, *Appl. Phys. A: Mater. Sci. Process.*, 2012, **107**, 421–428.
3 M. Cuscuna, A. Convertino, E. Zampetti, A. Macagnano, A. Pecora, G. Fortunato, L. Felisari, G. Nicorta, C. Spinella and F. Martelli, *Appl. Phys. Lett.*, 2012, **101**, 103101.
4 Z. Li, Y. Chen, X. Li, T. I. Kamins, K. Nauka and R. S. Williams, *Nano Lett.*, 2004, **4**, 245–247.
5 Y. Cui, Q. Q. Wei, H. K. Park and C. M. Lieber, *Science*, 2001, **293**, 1289–1292.
6 G. Zheng, F. Patolsky, Y. Cui, W. U. Wang and C. M. Lieber, *Nat. Biotechnol.*, 2005, **23**, 1294–1301.
7 F. Patolsky, G. F. Zheng, O. Hayden, M. Lakadamyali, X. W. Zhuang and C. M. Lieber, *Proc. Natl. Acad. Sci. U. S. A.*, 2004, **101**, 14017–14022.
8 N. Misra, J. A. Marinez, S. J. Huang, Y. Wang, P. Stroeve, C. P. Grigoropoulos and A. Noy, *Proc. Natl. Acad. Sci. U. S. A.*, 2009, **106**, 13780–13784.
9 R. G. Nuzzo and D. L. Allara, *J. Am. Chem. Soc.*, 1983, **105**, 4481–4483.
10 J. H. Lim, D. S. Ginger, K. B. Lee, J. S. Heo, J. M. Nam and C. A. Mirkin, *Angew. Chem., Int. Ed.*, 2003, **42**, 2309–2312.
11 Z. M. Fresco and J. M. Frechet, *J. Am. Chem. Soc.*, 2005, **127**, 8302–8303.
12 N. Naujoks and A. Stemmer, *Microelectron. Eng.*, 2003, **67–68**, 736–741.
13 J. P. Renault, A. Bernard, A. Bernard, D. Juncker, B. Michel, H. R. Bosshard and E. Delamarche, *Angew. Chem., Int. Ed.*, 2002, **41**, 2320–2323.
14 J. P. Renault, A. Bernard, A. Bietsch, B. Michel, H. R. Bosshard, E. Delamarche, M. Kreiter, B. Hecht and U. P. Wild, *J. Phys. Chem. B*, 2003, **107**, 703–711.
15 I. Park, Z. Li, A. P. Pisano and R. S. Williams, *Nano Lett.*, 2007, **7**, 3106–3111.
16 C. Y. Jin, Z. Li, R. S. Williams, K.-C. Lee and I. Park, *Nano Lett.*, 2011, **11**, 4818–4825.
17 M. Lim, D. Kim, C. O. Park, Y. Lee, S. W. Han, Z. Li, R. S. Williams and I. Park, *ACS Nano*, 2012, **6**, 598–608.
18 P. Norton and J. Brandt, *Solid-State Electron.*, 1978, **21**, 969–974.
19 N. Kularatna, *Digital and analogue instrumentation testing and measurement*, The institution of engineering and technology, London, 2008.
20 F. Ruffino, A. Irrera, R. De Bastiani and M. G. Grimaldi, *J. Appl. Phys.*, 2009, **106**, 084309.
21 R. Dus, E. Nowicka and Z. Wolfram, *Surf. Sci.*, 1989, **216**, 1–13.
22 R. J. Wolf, M. W. Lee and R. C. Davis, *Phys. Rev. B: Condens. Matter Mater. Phys.*, 1993, **48**, 12415–12418.

